ЖУРНАЛ СТРУКТУРНОЙ ХИМИИ

2015. Том 56, № 7 *Декабрь* *С. 1457 – 1462*

UDC 547.53:548.73:543.422

STRUCTURAL CHARACTERIZATION AND NONLINEAR OPTICAL PROPERTIES OF 1-PHENYL-3-(4-bis(2-CHLOROETHYL)AMINOPHENYL)-2-PROPEN-1-ONE

Anitha Sankaraperumal[1], A.N. Shetty[2], J. Karthikeyan[1]

[1]*Department of Chemistry, Sathyabama University, Chennai, India*
E-mail: dr.j.karthikeyan@gmail.com; jkarthik_chem@rediffmail.com (J. Karthikeyan)
[2]*Department of Chemistry, National Institute of Technology Karnataka, Mangalore, India*

Received November, 8, 2013 *Revised — August, 22, 2014*

A new chalcone derivative 1-phenyl-3-(4-bis(2-chloroethyl)aminophenyl)-2-propen-1-one with the molecular formula $C_{19}H_{19}Cl_2NO$ is synthesized by the Claisen—Schmidt condensation reaction. A transparent yellow single crystal was obtained by the slow evaporation solution growth technique using ethanol at room temperature. The compound crystallizes in the triclinic crystal system, *P*-1 space group, $Z = 4$, calculated density = 1.332 mg/m^3, V = = 1736.00(8) Å^3 with unit cell parameters $a = 7.8899(2)$ Å, $b = 14.1924(4)$ Å, $c = 15.7879(4)$ Å, $\alpha = 83.1280(10)°$, $\beta = 81.929(2)°$, $\gamma = 86.4820°$. The second harmonic generation efficiency is found to be 1.5 times higher than that of urea. Thermal stability of the crystal is found to be 250 °C determined from the thermogravimetric analysis. The FT-IR spectroscopy is used to identify the functional groups of the synthesized compound. The optical behavior of the grown crystal is examined by the UV-visible spectral analysis, which shows that the absorbance is almost negligible in the wavelength range 400—1300 nm.

DOI: 10.15372/JSC20150722

K e y w o r d s: synthesis, optical materials, chemical synthesis,crystal growth, X-ray diffraction, infrared spectroscopy, crystal structure.

INTRODUCTION

Organic crystals with large nonlinear optical (NLO) susceptibilities attract great interest due to their potential applications in second harmonic generation, including optical switching, eye and sensor protection. Recently, organic crystals have been highly recognized as the materials of the future because of their molecular nature and a possibility to alter their structure in order to maximize the nonlinear properties. Among various organic compounds reported for the nonlinear optical (NLO) properties, chalcones [1, 2] have received considerable interest as materials for second order NLO applications due to their ability to crystallize in a non-centrosymmetric structure and their blue light transmittance. Generally, molecular organic compounds with one or more aromatic systems in the conjugated position leading to charge transfer systems and with high optical nonlinearity are proposed as promising materials for future optoelectronic and NLO applications because these molecules have been found to originate from a strong delocalization of π-electrons along the length of the molecules, crystallizing in the non-centrosymmetric class [3]. Moreover, it is observed that in order to improve the activity a more bulky substituent should be introduced to increase the spontaneous polarization of a centric crystal. The molecular hyperpolarizability (β) is strongly influenced not only by the electronic effect but also by the steric effect of the substituent [4]. Prompted by this and in continuation of our quest, we report the growth of a new promising nonlinear organic single crystal: 1-phenyl-3-(4-

bis(2-chloroethyl)aminophenyl)-2-propen-1-one (CEAB-C). We have grown this crystal by the low temperature solution growth technique. The crystal was characterized by single crystal XRD, FTIR, TGA, DTA, UV-Visible spectroscopy and its SHG efficiency is discussed in this paper.

EXPERIMENTAL

Materials. All reagents and reactants were of analytical grade. The starting material p-[N,N-bis(2-chloroethyl)amino]benzaldehyde was prepared by the reported procedure [5]. The purity of the compound was checked by the elemental analysis and the melting point. Acetophenone, ethanol, NaOH were purchased from Merck (India) and used as received.

Measurements. Infrared spectral measurements were performed on a Shimadzu DR 8001 series FTIR instrument using KBr pellets for spectra in the range 4000—400 cm^{-1}, and FTIR spectra were recorded using polyethylene pellets on a Nicolet Magna 550 FTIR instrument in the range 500—100 cm^{-1}. An Ocean Optics SD 2000 Fiber Optic UV spectrophotometer was used to measure spectra in the range 200—900 nm. ^1H NMR spectra were recorded using an AMX 400 MHz FT-NMR spectrometer with d^6-DMSO as a solvent.

Preparation of 1-phenyl-3-(4-bis(2-chloroethyl)amino phenyl)-2-propen-1-one. The starting material *p*-[N,N-bis(2-chloroethyl)amino]benzaldehyde was prepared by the reported procedure [5]. The purity of the compound was checked by the elemental analysis and the melting point. The new chalcone was synthesized by the condensation of equimolar quantities of (Claisen-Schmidt condensation) *p*-[N,N-bis(2-chloroethyl)amino]benzaldehyde with acetophenone in ethanol. To this solution sodium hydroxide (10 %, 5 ml) was added and the reaction mixture stirred for 45 min and kept in the refrigerator overnight. The chalcones obtained were purified by recrystallisation using ethanol. Light yellow crystals suitable for X-ray diffraction studies were obtained by slow evaporation of its ethanol solution at room temperature. The reaction scheme is shown in Fig. 1.

Spectral studies. UV-Visible spectra. The UV-Visible spectra of the compound show a strong absorption band in the UV region, transparent in the entire visible region, and exhibit solvatochromism i.e. its maximum absorption peaks show bathochromic behavior with a band shift less than 400 nm. The absorption maximum for CEAB-C at 399 nm was assigned to the *n*—π* transition and can be attributed to the excitation in the aromatic ring and the C=O group, generally considered to be indicative of first molecular hyper polarizabilities with a non-zero value [6, 7]. The absence of absorption peaks in the visible region suggests that CEAB-C should be highly suitable for NLO application. The UV-Visible spectrum of CEAB-C is shown in Fig. 2.

FTIR spectra. The FTIR analysis of CEAB-C was carried out in the range 400—4000 cm^{-1}. The spectrum is shown in Fig. 3. FTIR spectroscopy is effectively used to identify the functional groups to determine the molecular structure of the synthesized compound. The various functional groups present in the CEAB-C compound were identified, and the chemical structure was confirmed by recording the IR spectrum. The characteristic IR absorption bands observed are consistent with the functional groups present in the compound and the assigned values are as those recorded in Table 1.

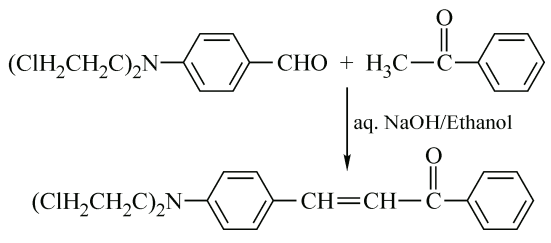

Fig. 1. Reaction scheme for the preparation of CEAB-C

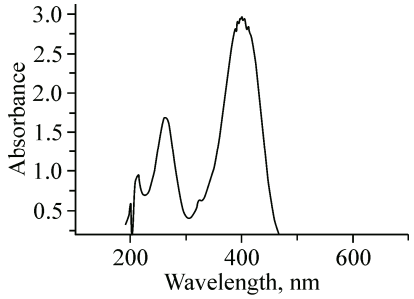

Fig. 2. Linear absorption UV-Visible spectrum of CEAB-C

NMR spectra. The NMR spectrum was recorded to confirm the presence of various types of protons and for the confirmation of the target compound. The H^1NMR data of CEAB-C shows multiplets at δ = 6.60—7.24 ppm corresponding to phenyl protons. The signals due to the —CH_2—CH_2— protons give multiplets at δ = 3.00—3.80 ppm. Two chalcone protons appearing at δ = 7.29(d, 1H, H-α) and δ = 7.43(d, 1H, H-β) confirm the presence of α,β unsaturated *trans*-alkene (—CH=CH—, *E*-form) in the compound [8].

T a b l e 1

Observed IR spectral data and their assignment in the range 4000—400 cm^{-1}

Bond type	Observed Frequency for CEAB-C, cm^{-1}
—C—H...O(Intramolecular hydrogen bonding)	3418
—CH_2 stretching	2888
Aromatic —N—C stretching	2165
—C=O stretching	1646
Aromatic —C=C— stretching	1467
—C—Cl stretching	962
Aromatic *para*-disubstituted benzene	841
—C—C=O in-plane deformation	528

RESULTS AND DISCUSSION

X-ray crystallography. Unit cell determination of the complex. The X-ray diffraction study was carried out using a Bruker AXS Kappa Apx II CCD single crystal diffractometer with MoK_α (λ = 0.7107 Å) radiation. The diffractometer is equipped with a four-circle goniometer with φ, χ, ω and 2θ axes by which the crystal is rotated. A crystal specimen with the dimensions of 0.30×0.30× ×0.25 mm was cut and mounted on a glass fiber using cyano acrylate. The unit cell parameters were determined by collecting the diffracted intensities from 36 frames measured in three different crystallographic zones and using the method of difference vectors followed by data collection at 293 K using ω—φ scan modes.

Structure solution and refinement of the complex. The structure was solved by direct methods using the SHELXS 97 program [9], which revealed the positions of all non-hydrogen atoms, and refined on F^2 by the full matrix least squares procedure using SHELXL 97. The non-hydrogen atoms were refined anisotropically and the hydrogen atoms were allowed to ride over their parent atoms. The final cycle of the refinement converged to $R_1 = 0.0392$ and $wR_2 = 0.0905$ for the observed reflections. The maximum and minimum heights in the final difference Fourier map were found to be 0.368 e/Å^{-3}

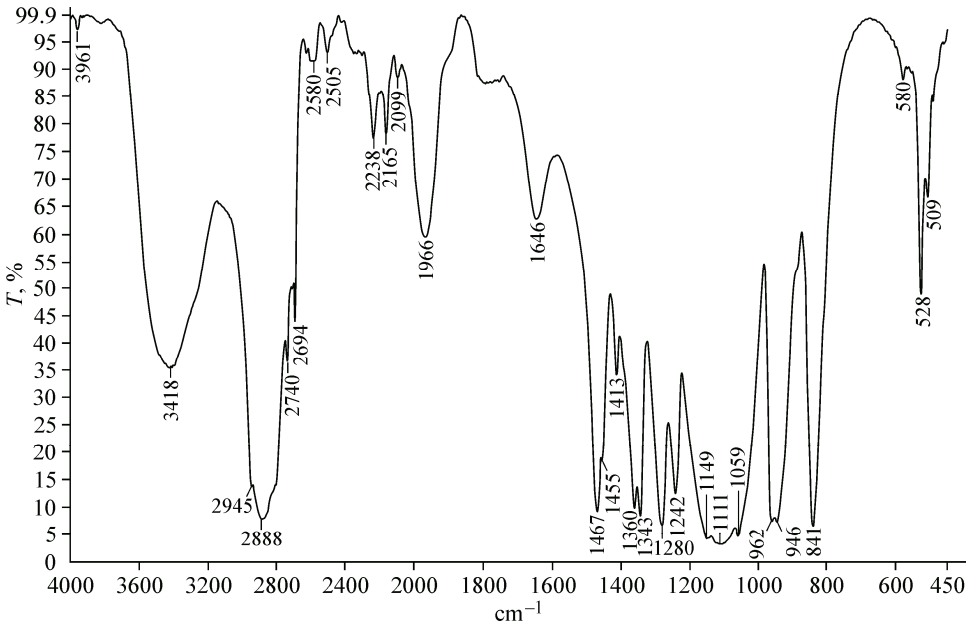

Fig. 3. FTIR spectrum of CEAB-C

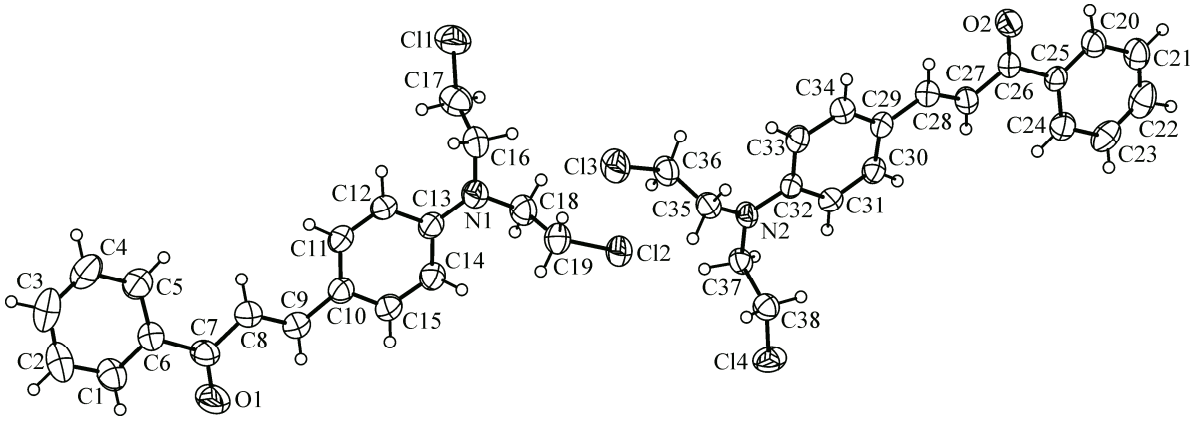

Fig. 4. Molecular structure of CEAB-C from the single crystal X-ray analysis

and –0.334 e/Å^{-3} respectively. Least squares plane and asymmetry calculations were made using the PARST 97 program. The thermal ellipsoid plot and packing were made using ORTEP and PLATON respectively [10, 11]. Non-bonded interaction graphics were created using the PLATON program. The crystallographic data and methods of data collection, bond distances, atomic coordinates, and equivalent isotropic displacement coefficients are included in the deposited material (CCDC-900263) as a complete list of bond distances and angles.

Crystal structure and packing features. In the title compound CEAB-C with the molecular formula $C_{19}H_{19}Cl_2NO$ crystallizes in the triclinic system with the space group *P*-1, *Z* = 4, calculated density = 1.332 mg/m^3, *V* = 1736.00(8) Å^3 with unit cell parameters *a* = 7.8899(2) Å, *b* = 14.1924(4) Å, *c* = 15.7879(4) Å, α = 83.1280(10)°, β = 81.929(2)°, γ = 86.4820(10)°; final R_1 and wR_2 are 0.0392 and 0.0905 respectively. The compound exists in stable *E*-form with respect to the C7=C8 and C27=C28 part [12]. In the compound, the C1—C6, C29—C34 rings are perfectly planar and the C10—C15, C20—C25 rings deviate significantly from planarity. The molecule as a whole does not deviate significantly from planarity. Dihedral angles between the constituent planar fragments are relatively small. The bis(2-chloroethyl)amino substituent and the α, β-unsaturated carbonyl group are almost coplanar with respect to the aromatic ring and also inclined with respect to the aromatic ring plane by 3.1(6)°. Two benzene rings are oriented at a dihedral angle of 10.59°. The torsion angle of the O(1)—C(7)—C(8)—C(9) moiety is 3.1(4)°. In the CEAB-C molecule the bond lengths of the C10—C15 and C29—C34 rings are considerably higher than the normal value of 1.37 Å by ±3σ. These are attributed to the resonance character of ethyl amine. The bond length variations of the phenyl ring confirm that the extended electron conjugation is observed between the central —CH=CH—C(=O)— group and the bis(2-chloroethyl)amino benzene ring [13], which was further confirmed by that the C(phenyl)—C(carbonyl) bond is considerably shorter 1.486(3) than those in P-aminoacetophenone. Fig. 4 presents ORTEP of the CEAB-C molecule with thermal ellipsoids at a 50 % probability level. In the crystal, the molecules are linked through intermolecular C36—H(36B)…O(1), C(20)—H(20)…Cl(2) and C(16)—H(16A)…Cl(3) hydrogen bonds, generating the edge-fused ring motif. The hydrogen bond motifs are linked to each other to form a three dimensional network, which seems to be effective in the stabilization of the crystal structure forming chains [14]. The crystal packing arrangement of CEAB-C is shown in Fig. 5. An intermolecular C—H…O (carbonyl) hydrogen bond favors the endo-conformation of the molecule. The dimensions of the hydrogen bonds are listed in Table 2.

T a b l e 2

Dimensions of hydrogen bonds for CEAB-C

D—H...A	*d*(D—H)	*d*(H...A)	*d*(D...A)	∠(DHA)
C(36)—H(36B)...O(1)$^{\#1}$	0.97	2.57	3.461(3)	152.8
C(20)—H(20)...Cl(2)$^{\#1}$	0.93	2.87	3.773(3)	165.4
C(16)—H(16A)...Cl(3)$^{\#1}$	0.97	2.88	3.783(3)	155.9

Nonlinear optical studies. The Kurtz and Perry powder relative SHG efficiency measurement technique was employed to determine

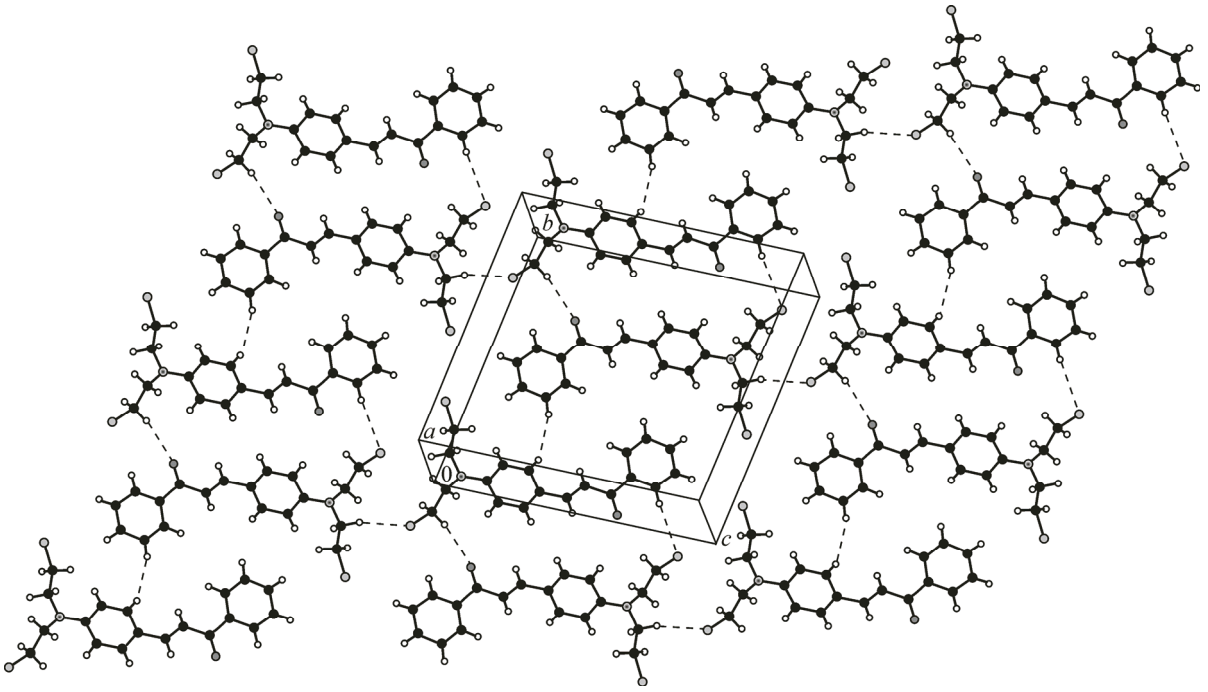

Fig. 5. Crystal packing arrangement of CEAB-C

the SHG efficiency [15] of CEAB-C. A Q-switched 7th Nd:YAG laser operating at 1064 nm with a 10 Hz repetition rate and a 3.4 mJ/pulse energy was used as light source in our experiment. CEAB-C and reference KDP and urea samples, pulverized to have an identical particle size of less than 63 μm, were filled in separate capillary tubes. A tight packing of the sample was ensured with the aid of a mechanical vibrator. The capillary tube was kept 3 cm away from the focused spot of the laser beam in order to avoid any laser-induced damage of the sample. The SHG signal from the sample was measured at an angle of 90° with respect to the laser beam direction. The fundamental light was filtered with the aid of a monochromator. The second harmonic signal was converted into the electrical signal using a photomultiplier tube and was finally displayed on a digital storage oscilloscope. The SHG output was averaged over 300 laser pulses. The SHG signal measured for standard KDP and urea was used for comparison with CEAB-C for the SHG experiments. For a laser input pulse of 3.4 mJ, the second harmonic signal of 16 mV, 178 mV, and 275 mV respectively were obtained using KDP, urea, and CEAB-C samples. Thus, the SHG efficiency of CEAB-C is 17 times higher than KDP and 1.5 times higher than that of urea.

Thermal studies. The thermal analysis of the material gives useful information regarding the thermal stability of that material. Despite their high SHG efficiency, organic crystals, when compared to inorganic crystals, have poor thermal and mechanical stabilities. To find the thermal stability of CEAB-C, the thermo gravimetric analysis was carried out. A powdered sample of the crystal was selected for this purpose and the analysis was carried out in the nitrogen atmosphere at a heating rate of 10°/min using a Perkin—Elmer simultaneous TGA/DTA analyzer. The result obtained from this analysis is depicted in Fig. 6. In the DTA curve, the endother mic peak observed at 95.15 °C corresponds to the melting point of CEAB-C, and the same has been verified using the capillary melting point appa-

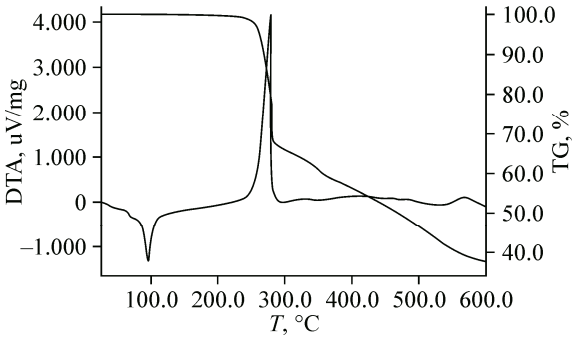

Fig. 6. TGA/DTA curve of CEAB-C

ratus. Note that no weight loss was observed in the TG curve at this melting point endotherm. The initial weight loss observed in the TG curve, which starts approximately at 230 °C, was due to the sublimation of CEAB-C. A major weight loss due to the sample decomposition was observed at around 250 °C and continued up to 600 °C. A sharp exothermic peak corresponding to the CEAB-C decomposition was observed at 275 °C. Thus, CEAB-C was thermally stable without any decomposition up to 250 °C above which the weight loss of sample began.

Micro-hardness test. The mechanical strength of the crystal was found by the Vickers microhardness method. The variation of the Vickers hardness number with an applied load was carried out on the (0 1 0) plate of CEAB-C crystals having a thickness of 1 mm. The diagonal length of the indented impression was measured for different loads. The plot indicates that the crystal hardness decreases with increasing load. The decrease in the micro-hardness with increasing load is in agreement with the normal indentation size effect [16]. By plotting log P versus log d, the value of the work hardening coefficient n was found to be 1.49. According to Onitsch, $1.0 \leq n \leq 1.6$ for hard materials and $n \geq 1.6$ for soft materials, based on Kick′s correlation ($P = kd^n$) [17]. Hence, it is concluded that CEAB-C is a hard material.

Chemical stability. In order to check the chemical stability of CEAB-C, a few crystals were kept in a polythene pouch and kept aside in the lab for more than six months. No significant change was observed in the crystal quality, indicating that the crystal was resistant to environmental variation and was chemically stable, unlike urea that is hygroscopic.

Laser damage studies. Suitability of organic crystals for optical studies depends not only on NLO properties, but largely on its ability to withstand high power lasers, otherwise its performance limits in NLO applications [18]. The CEAB-C crystal was investigated for a single shot surface damage for 1064 nm laser radiation using a Q-switched Nd:YAG laser with a pulse width of 9 ns and a 10 Hz repetition rate. For this measurement, a 5 mm diameter beam is focused on the sample with a 6 cm focal length lens. It is observed that the CEAB-C crystal has a moderate damage threshold of 3.56 GW/cm^2.

All crystallographic data for this paper are deposited with the Cambridge Crystallographic Data Centre [CCDC-900263]. The data can be obtained free of charge at www.ccdc.cam.ac.uk/conts/retrieving.html [or from Cambridge Crystallographic Data Centre (CCDC), 12 Union Road, Cambridge CB2 1EZ, UK, fax: +44 (0) 1223-336033, e-mail:deposit@ccdc.cam.ac.uk.

REFERENCES

1. *Zhang G.J., Kinoshita T., Sasaki K., Goto Y., Nakayama Y. et al.* // Appl. Phys. Lett. – 1990. – **57**. – P. 221 – 224.
2. *Indira J., Karath P.P., Sarojini B.K. et al.* // J. Cryst. Growth. – 2002. – **242**. – P. 209 – 214.
3. *Goto Y., Hyashi A., Kimura Y., Naakayama S.M. et al.* // J. Cryst. Growth. – 1991. – **108**. – P. 688 – 698.
4. *Cho B.R., Je J.T., Kim H.S., Jean S.J., Song O.K., Wang C.H. et al.* // Bull. Korean Chem. Soc. – 1996. – **17**. – P. 693 – 695.
5. *Elderfield R.C., Covey I.S., Geiduschek J.B., Meyer W.L., Ross A.B., Ross J.H. et al.* // Potential Anticancer Agents. – 1958. – **23**. – P. 1749 – 1753.
6. *Zhou Y. et al.* // Mat. Sci. Eng. B. – 2003. – **99**. – P. 593 – 596.
7. *Albert I.D.L., Marks T.J., Ratner M.A. et al.* // Chem. Mater. – 1998. – **10**. – P. 753 – 762.
8. *Rojas J., Domínguez J.N., Charris J.E., Lobo G., Payá M., Ferrándiz M.L. et al*. // Eur. J. Med. Chem. – 2002. – **37**. – P. 699 – 705.
9. *Sheldrick G.M. et al.* // Acta Crystallogr. – 2008. – **A64**. – P. 112 – 122.
10. *Farrugia L.J. et al.* // J. Appl. Crystallogr. – 1997. – **30**. – P. 565 – 569.
11. *Spek A.L. et al.* PLATON, A Multipurpose Crystallographic Tool; Utrecht University: Utrecht, Netherlands, 1999.
12. *Noyce D.C., Pryor W.A., King P.A. et al.* // J. Am. Chem. Soc. – 1959. – **81**. – P. 5423 – 5428.
13. *Varanasi P.R., Jen A.K.Y., Chandrasekhar J., Namboothiri I.N.N., Rathna A. et al.* // J. Am. Chem. Soc. – 1996. – **118**. – P. 12443 – 12448.
14. *Hao Y.-M. et al.* // Acta Crystallogr. – 2010. – **E66**. – P. 2528.
15. *Kurtz S.K., Perry T.T. et al.* // J. Appl. Phys. – 1968. – **39**. – P. 3728.
16. *Subhadra K.G., KisnanRao K., Sirdeshmukh D.B. et al.* // Bull. Mater. Sci. – 2000. – **23**. – P. 147 – 150.
17. *Mukerji S., Kar T. et al.* // Cryst. Res. Technol. – 1999. – **34**. – P. 1323.
18. *Bhar G.C., Chaudhury A.K., Kumbhakar P. et al.* // Appl. Surf. Sci. – 2000. – **161**. – P. 155 – 162.